

# Q-score Max-Clique: The First Quantum Metric Evaluation on Multiple Computational Paradigms

Ward van der Schoot      Robert Wezeman  
Niels M. P. Neumann      Frank Phillipson      Rob Kooij

February 2, 2023

## Abstract

Evaluating the performance of quantum devices is an important step towards scaling quantum devices and eventually using them in practice. The great number of available quantum metrics and the different hardware technologies used to develop quantum computers complicate this evaluation. In addition, different computational paradigms implement quantum operations in different ways. We add to the landscape of quantum metrics by extending the Q-score metric of Atos to the Q-score Max-Clique. To our knowledge, this yields the first application-level metric which allows comparison of different paradigms of quantum computing. This metric is evaluated on three different computational quantum paradigms – quantum annealing, gate-based quantum computing, and photonic quantum computing – and the results are compared to those obtained by classical solvers.

## 1 Introduction

Quantum computers have been under constant development over the last few years and both industry and academia have made tremendous efforts to build ever more powerful quantum computers. The efforts are however diverse, as there is no consensus on the best approach to building qubits, the fundamental computational units of a quantum computer. So far, qubits have been based on various physical phenomena, such as superconductivity [6, 22, 27], trapped ions [8] and photons [31]. Moreover, no consensus exists on the best paradigm for quantum computing. Three well-known approaches are quantum annealing, gate-based quantum computing and photonic quantum computing. Each hardware technology and even each computational paradigm has its own pros and cons that make it suitable for specific applications.

While comparing quantum devices based on the same technology is already hard, comparing quantum devices based on different technologies is a research field on its own. *Quantum metrics* provide a first step towards quantifying the performance of quantum devices in a unified manner. However, just as with

quantum computers, a single best metric does not exist. Instead, there exist multiple metrics and each has its own benefits and limitations.

For a long time, quantum devices were compared based on physical characteristics, such as global and single qubit coherence times and gate operation times, for instance by means of randomized benchmarking [10, 12]. While these numbers give valuable insights into the physical performance of a system, they do not necessarily say much about the performance of a quantum system.

The quantum volume metric [9] tries to overcome this difficulty by measuring the performance of a quantum device at implementing quantum circuits. Complementary to the quantum volume metric, there is the CLOPS metric, which measures the time required to implement these circuits [37]. Both the quantum volume and the CLOPS metric output a single value, which makes comparing the value relatively easy. However, these metrics can only be used to benchmark gate-based quantum devices. Moreover, their output says relatively little on the capabilities of solving practical problems.

Application-level metrics address the latter issue by measuring the performance of quantum devices on quantum algorithms and practical problems. An example is given by the suite of the QED Consortium [25], which considers a few standard quantum algorithms to compare the performance of quantum devices. While this application-level metric gives insight in the performance of the quantum device, it is still only applicable to gate-based devices. This is reasonable, as gate-based quantum computers have the promise to be universal [2, 7]. However, other quantum computational paradigms such as photonic quantum computing and quantum annealing are also relevant and useful for specific problems.

This issue is solved by the Q-score metric because it is computing paradigm agnostic [28]. In addition, the Q-score can be computed for classical algorithms, which allows direct comparison with classical alternatives. The main idea behind the Q-score metric is that a quantum routine usually is part of a larger computational workflow and benchmarks should therefore consider the whole computational pipeline instead of only the quantum part.

In this work, we extend the original formulation of the Q-score to define the Q-score Max-Clique, which allows comparison of quantum annealers, gate-based and photonic quantum devices. We use it to benchmark these three computational paradigms, as well as two classical solvers. To our knowledge, this is the first time performance of these four computational paradigms is compared.

The structure of this paper is as follows: In Section 2 background information is provided on quantum computing for different technology paradigms and earlier Q-score work. Section 3 defines the Q-score Max-Clique metric and Section 4 presents the experiments and subsequent results. This work concludes with a discussion of the results and directions for further research in Section 5.

## 2 Background

### 2.1 Quantum Computing

Quantum computers exploit quantum mechanical principles to perform operations and solve problems. Contrary to classical states, quantum states do not have to be in a single computational basis state. Instead, a quantum state can be any complex linear combination of multiple computational basis states, a so-called superposition. Upon measurement, only a single computational basis state is found and the probability depends on the amplitude of that state right before the measurement. In addition, quantum states exhibit correlations beyond what is possible classically. This strong correlation between quantum states is called entanglement.

No consensus exists on how quantum computers should best exploit these principles. Some approaches can perform general computations but are harder to build or scale, while other techniques might be easier to implement but are limited in the type of problems they can handle. The next three sections briefly recap three popular approaches to quantum computing.

#### 2.1.1 Quantum annealing

Quantum annealing is based on a different form of quantum computing called adiabatic quantum computing [16], which is known to be equivalent to standard gate-based quantum computing [3]. In adiabatic quantum computing qubits are not addressed individually, but, instead, qubits are prepared in some initial state and a certain Hamiltonian is slowly applied to these qubits. The Hamiltonian is constructed so that its ground-state encodes the solution of the problem. If this evolution is slow enough, the state remains in the ground state of the Hamiltonian throughout evolution, yielding the solution to the problem. The system is required to remain coherent during the evolution time. As this evolution time of the process can be exponential in the size of the problem, there are certain limitations to adiabatic quantum computing.

Quantum annealing tries to solve precisely this problem [23], where the Hamiltonian is applied fast and more often. While the system is unlikely to remain in the ground-state, more samples get generated, which can approximate the ground-state reasonably well. In its current form, quantum annealing is non-universal and only suited for optimisation problems. Programming quantum annealing algorithms requires describing the algorithm as a quadratic unconstrained binary optimisation (QUBO) problem. Many problems have a QUBO formulation [26] and have been implemented on available hardware for small problem instances.

#### 2.1.2 Gate-based quantum computing

Gate-based quantum computing comes closest to classical digital computers. Individual qubits or groups of qubits are manipulated by means of quantum gates. By careful manipulation of the right qubits, any unitary operation can

be implemented on these qubits. Because of its similarity to classical computers, any classical computing circuit can also be run on a gate-based quantum device. However, most gate-based devices are limited to single qubit gates and specific two-qubit gates on adjacent qubits. While this limits the unitary operations a device can perform, this suffices for approximating any unitary operation to arbitrary precision [24].

### 2.1.3 Photonic quantum computing

With photonic hardware, photons are used as qubits. Photonic quantum devices manipulate these photons using phase shifters and beamsplitters. Phase shifters changes the phase of the light, whereas beamsplitters entangles two different light waves. Finally, squeezers change the position and the momentum of the light wave. This is a non-linear interaction needed for universal quantum computing. In theory universal computations are possible on photonic quantum devices. However, a main limitation is that universal computations using photonic devices require probabilistic non-linear interactions. Because of this, there is only a certain probability of successfully running the algorithm. The depth of circuits that are performed on photonic quantum devices are inherently limited by the length of the used setup. To overcome this, some form of rerouting the photons back into the setup while simultaneously changing the operations and the next path for the photons would be needed. Currently, this has not yet been implemented in practice.

## 2.2 Q-score

In 2021, the company Atos proposed the original Q-score metric with the idea that the state-of-the-art benchmarking of quantum devices was insufficient to assess High-Performance Computing platforms [28]. They designed the Q-score with the idea of having a metric which is: “application-centric, hardware-agnostic and scalable to quantum advantage processor sizes and beyond”.

In its original definition, the Q-score measures the largest average problem instance of the Max-Cut problem at which a (quantum) device significantly outperforms a random algorithm. The Max-Cut problem is an NP-hard problem in graph theory which entails finding a partition  $P$  of the vertices of a (weighted) graph into two sets, so that the total weight of edges between the two sets is maximal. The partition  $P$  is called a cut and the total weight between these two sets is called the cost  $C(P)$ . Just like many optimisation problems, the Max-Cut problem has a QUBO formulation. In addition, the Max-Cut problem is shown to be equivalent to many other optimisation problems. The Q-score can thus be seen as a metric that measures the performance of a (quantum) device on optimisation problems.

To gauge the performance of a certain device on the Max-Cut problem, Atos suggests solving the Max-Cut problem for  $(N, \frac{1}{2})$ -Erdős-Rényi graphs  $G$  [13, 14], which are graphs with  $N$  vertices in which each edge exists with probability  $\frac{1}{2}$ . By running the algorithm on sufficiently many random graph instances, the

average best cut  $C(N)$  can be computed. This value is then compared to both the average cost of a random cut  $C_{rand}$  on the same graphs and the average cost of the best cut  $C_{max}$  of the same graphs. The performance of the obtained solution can then be gauged by evaluating the function  $\beta(N)$ :

$$\beta(N) = \frac{C(N) - C_{rand}}{C_{max} - C_{rand}} = \frac{C(N) - N^2/8}{0.178N^{3/2}},$$

The expression  $C_{rand} = N^2/8$  is based upon a random algorithm which randomly partitions the vertices into two sets of size  $\lfloor \frac{N}{2} \rfloor$  and  $\lceil \frac{N}{2} \rceil$ . As each edge exists with probability  $\frac{1}{2}$ , the expected cost of this cut is  $\lfloor \frac{N}{2} \rfloor \cdot \lceil \frac{N}{2} \rceil \cdot \frac{1}{2} \approx \frac{N^2}{8}$ . The expression  $C_{max} = N^2/8 + 0.178N^{3/2}$  follows from theoretical results and a least-squared numerical fit for smaller values of  $N$  [28].

From the definition of  $\beta(N)$  it follows that a random approach approximately results in a  $\beta(N)$  of roughly zero. In contrast, an algorithm that always finds the best possible cut will give  $\beta(N) \approx 1$ . The value  $\beta(N)$  hence captures how ‘good’ a cut is, with higher  $\beta(N)$  values corresponding to better cuts. The Q-score of a device is defined as the largest  $N$  for which  $\beta(N) > \beta^*$ , for some threshold value  $\beta^*$ .

Atos suggest a threshold value  $\beta^* = 0.2$  to represent a successful execution of the algorithm. Thus, any algorithm achieving a  $\beta(N)$  value higher than 0.2 successfully solved the problem. Other choices might suffice as well, however  $\beta^* = 0.2$  is chosen so that a noiseless gate-based quantum device running the Quantum Approximate Optimisation Algorithm (QAOA) [15] with  $p = 1$  obtains an infinite Q-score.

Any device that can solve the Max-Cut problem can be assigned a Q-score. This includes classical devices, gate-based quantum computers and quantum annealing devices. The Q-score hence allows for comparing devices based on different computational paradigms. Note that the Q-score depends not only on the used backend device, but also on the used algorithm, which gives freedom to use different algorithms and also compare them to each other. Naturally, this calls for mentioning the used algorithm to compute the Q-score.

The original definition of the Q-score allows the user to choose some variables, such as the allowed time for the computation. This impacts the Q-score significantly, as classical devices can solve the problem for any  $N$  perfectly given a sufficient amount of time. Other examples of user-variables to choose are the number of random instances of  $(N, \frac{1}{2})$ -Erdős-Rényi graph instances and the allowed pre- and post-processing optimisation steps. Earlier work [36] imposed a time-constraint of at most 60 seconds for each instance, a total of 100 random graph instances per graph size and considered each solver in an out-of-the-box fashion to restrict any pre- or post-processing optimisation steps. If a device failed to find an answer within 60 seconds, a random cut was used for that instance, corresponding to a value of  $\beta(N) = 0$ . This earlier work showed that, given these constraints, classical backends achieve higher Q-scores (2,300 and 5,800) than state-of-the-art quantum annealing hardware (70 and 140). In turn, the offered hybrid method achieved a Q-score of 12,500, which hints at gains

offered by quantum annealing. [36] also briefly discusses gate-based devices and their expected lower Q-score, mainly due to their low number of available qubits, and does not discuss photonic devices.

### 3 The Q-score Max-Clique metric

This section introduces the Q-score Max-Clique metric: a new and improved version of the Q-score. This new metric takes the ideas of the Q-score and enhances them so that the metric can also be evaluated on photonic quantum devices, in addition to gate-based quantum devices, quantum annealers and classical devices.

Just like the Q-score, the Q-score Max-Clique aims to gauge the performance of a device by measuring the largest problem size  $N$  of a certain optimisation problem for which the device significantly outperforms a random solution. The *Max-Clique problem*, contrary to the Max-Cut problem, allows for a more natural comparison between all mentioned backends.

The Max-Clique problem is an established NP-hard problem in graph theory which aims to find the largest complete subgraph of a random graph of size  $N$ . A complete graph, or clique, is a graph in which every two vertices are connected by an edge. Just like the Max-Cut problem, the Max-Clique problem has a QUBO-formulation and the problem is hence equivalent to many optimisation problems, in particular to the Max-Cut problem [19]. The Q-score Max-Clique hence also serves as a metric on how well a device performs at optimisation problems.

For computing the Q-score Max-Clique, the same variables as for the original Q-score are used:  $(N, \frac{1}{2})$ -Erdős-Rényi graphs are considered and the cost  $C(N)$  is computed as the average clique size found over 100 random instance of these graphs. The value  $\beta(N)$  for this algorithm is then computed as

$$\beta(N) = \frac{C(N) - C_{rand}}{C_{max} - C_{rand}}.$$

Here,  $C_{rand}$  is the average clique size found by the following random naive approach: start with an empty sub-graph  $G'$ ; Take a random node  $v \in G \setminus G'$  and add this to  $G'$  if,  $G' \cup \{v\}$  is still a clique. If not, return the number of nodes in  $G'$  as the maximum clique size found by this random algorithm. For general  $(N, p)$ -Erdős-Rényi graphs, the probability that this naive algorithm finds a clique of size at least  $i$  is

$$\mathbb{P}[X \geq i] = p^{i(i-1)/2}.$$

This follows as each of the  $i(i-1)/2$  edges has to be present and each edge is added to the graph independently with probability  $p$ . From this it follows that

$$\mathbb{P}[X = i] = \mathbb{P}[X \geq i] - \mathbb{P}[X \geq i + 1] = p^{i(i-1)/2} - p^{i(i+1)/2} = (1 - p^i)p^{i(i-1)/2}.$$

The expected size of the clique found with the naive algorithm then equals

$$\mathbb{E}[X] = \sum_{i=1}^N i \cdot \mathbb{P}[X = i] = \sum_{i=1}^N i \cdot (1 - p^i)p^{i(i-1)/2}.$$

For  $p = \frac{1}{2}$ , this approximately gives  $C_{rand} = \mathbb{E}[X] = 1.6416325$ . Again,  $C_{max}$  is the actual maximum clique size of the graph, averaged over the 100 random instances. According to [29], this value scales as

$$C_{max} = 2 \log_2(N) - 2 \log_2(\log_2(N)) + 2 \log_2(e/2) + 1.$$

Note that this is an asymptotic result for  $N \rightarrow \infty$  and might not be a good approximation for smaller  $N$ .

A device significantly outperforms a random algorithm for some problem instance  $N$  if  $\beta(N) > \beta^*$ , where again  $\beta^* = 0.2$  is taken, following [11]. So a device outperforms a random algorithm if

$$\begin{aligned} \beta(N) &= \frac{C(N) - C_{rand}}{C_{max} - C_{rand}} \\ &= \frac{C(N) - 1.6416325}{2 \log_2(N) - 2 \log_2(\log_2(N)) + 2 \log_2(e/2) - 1.6416325} > 0.2. \end{aligned}$$

The limit on the computation time is set to 60 seconds per instance, as in [36]. If a device does not find an answer within the allocated 60 seconds, a clique size of  $C_{rand}$  is assigned, corresponding to a value of  $\beta(N) = 0$ . Finally, all algorithms are considered in an out-of-the-box fashion to restrict any additional optimisation steps.

## 4 Results

This section gives the Q-score Max-Clique results for different computational paradigms. First, a brief overview is given of how the Max-Clique problem can be solved on each of the quantum computing paradigms, as well as the devices for which the Q-score Max-Clique is computed.

- **Quantum Annealing:** A QUBO is formulated for the Max-Clique problem [19] and then then solved using annealing hardware from D-Wave Systems Inc. Both their 2000Q and Advantage systems, with 2041 qubits and 5627 qubits, respectively, are considered.
- **Gate-based quantum computing:** The same QUBO formulation can be used to solve Max-Clique instances using the Quantum Approximate Optimisation Algorithm (QAOA). Although gate-based hardware is being developed by a large variety of vendors, the devices are smaller than quantum annealers in terms of total number of qubits. Users can access the devices via the cloud, and hence resources are shared with other users.

Currently, each set of quantum circuits needs to be sent as a job through the entire stack and queue, which especially in variational settings is inefficient. Solutions are being developed that provide users the ability to avoid latency by executing entire programs in containerised services, such as Qiskit Runtime [33]. Still, significant queue times remain and once scheduled, a single problem instance can still take around an hour to execute in practice. The actual computation time QAOA would take with direct access to dedicated hardware is hard to estimate. A methodology to reason about the execution-time of QAOA is developed in [38]. According to their estimates, candidate solutions for Max-Cut graphs with 500 nodes can be generated in under three minutes, which is still above the 60 seconds threshold.

A simple QAOA implementation is considered using only one layer with SLSQP as optimisation algorithm, see [34] for the exact implementation. For the experiments, two hardware backends from different vendors are used: the 16 qubit Guadalupe device [32] by IBM, and the 5 qubit Starmon-5 device [35] by Quantum-Inspire. Additionally, noiseless simulations are performed to upper bound what real hardware can achieve.

- **Photonic quantum computing:** The main component used in photonic quantum computing to solve Max-Clique instances is called Boson sampling [1]. Boson sampling can be used to obtain dense subgraphs from a graph [4]. By removing the least-dense vertices of such subgraphs, they can be converted into cliques. Such a clique can be made maximal by adding fully connected vertices to it. It should be noted that the latter two steps are classical steps, making this algorithm a photonic-classical hybrid algorithm. It was shown that the resulting hybrid procedure is able to find maximal cliques with sufficiently high probability [5]. A more extensive overview of using boson sampling for solving Max-Clique problems can be found in [21].

In addition, the Q-score Max-Clique is also calculated for two classical solvers, namely qbsolv and simulated annealing, both offered by D-Wave Systems Inc. The qbsolv method solves smaller pieces of a QUBO with a tabu search algorithm [17, 18] and then combines those solutions to a full solution. The simulating annealing method is able to solve a QUBO by searching the solution space and slowly decreasing the probability of accepting worse solutions than the current optimum. Lastly, the Q-score Max-Clique is computed for the hybrid solver provided by D-Wave Systems Inc.. This is an algorithm which combines classical and annealing approaches to solve QUBOs. The precise workings of this solver are however unknown. Table 1 gives the Q-score of all considered backends.

## 4.1 Experiments

To compute the Q-score Max-Clique, 100 random  $(N, \frac{1}{2})$ -Erdős-Rényi graphs are generated for increasing problem sizes  $N$  with the NetworkX python library.



Table 1: Q-scores Max-Clique with a 60 seconds time limit.

Approach	Q-score	Approach	Simulated Q-score
Tabu search	4,900	QAOA	$\geq 16^*$
Simulated annealing	9,100	Photonics	$\geq 20^*$
D-Wave Advantage	110		
D-Wave 2000Q	70		
Hybrid solver	12,500		
Starmon-5 (QAOA)	5*		
IBM-Guadalupe (QAOA)	$\geq 5^*$		

Next, the Max-Clique problem for these graphs is solved by the different solvers in an out-of-the-box fashion with the imposed time constraint of 60 seconds. This time considers the entire computation time starting from either a graph or QUBO representation. The only exception is the QAOA algorithm, for which only 10 graph instances are considered and no time limit is imposed due to long queuing times. For the simulations of the gate-based and photonic approach the time constraint is also ignored as the simulation time does not represent the time it would take real hardware to solve the problem. After obtaining all results for the graphs, the average cost  $C(N)$  and corresponding  $\beta(N)$  are computed. The graph size  $N$  is increased until  $\beta(N) \leq 0.2$ . For the classical algorithms we use a modest server with an Intel Core i7-7600U CPU with a clock speed of 2.80GHz and 12 GBs of RAM. All code used to perform our experiments has been made open source and can be found at [34].

Below, the found results for each of the computational paradigms are discussed in detail.

- **Quantum Annealing:** The  $\beta$  vs  $N$  graph for the D-Wave Advantage device and its previous-generation 2000Q device are shown in Fig. 1. The experiments for both devices start at  $N = 5$  and in each new step, increase  $N$  by five. For the Advantage system,  $\beta = 0.2$  occurs for  $N = 110$ , which yields a Q-score Max-Clique of 110. For the 2000Q device it is not possible to find a problem embedding for instances larger than approximately  $N = 70$ . Hence, a Q-score Max-Clique of 70 is found. Interestingly, similar limitations exist for Q-score Max-Cut at the same problem size [36]. It should be noted that [30] deal with this issue by investigating methods for decomposing larger problem instances for Max-Clique into smaller ones, which can subsequently be solved on the 2000Q device.

For small  $N$ , the approximation  $C_{max}$  is suboptimal, which explains the counter-intuitive behaviour seen in the  $\beta$  vs  $N$  graph for small  $N$ . The crossing  $\beta = 0.2$  is unaffected by this approximation error. For completeness, Fig. 2 gives the  $\beta$  vs  $N$  graphs with  $C_{max}$  the actual largest clique, instead of an approximation value.

- **Gate-based quantum computing:** The Q-score Max-Clique was computed for two hardware backends up to problem sizes  $N = 5$ . On both the

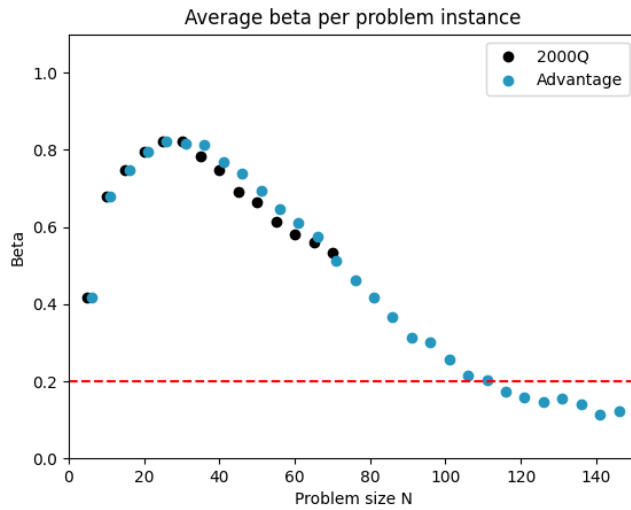


Figure 1: Max-Clique Q-score's  $\beta$  vs problem size  $N$  for the D-wave Advantage and 2000Q QPUs. For visibility reasons, the advantage graph is off-set by 1.

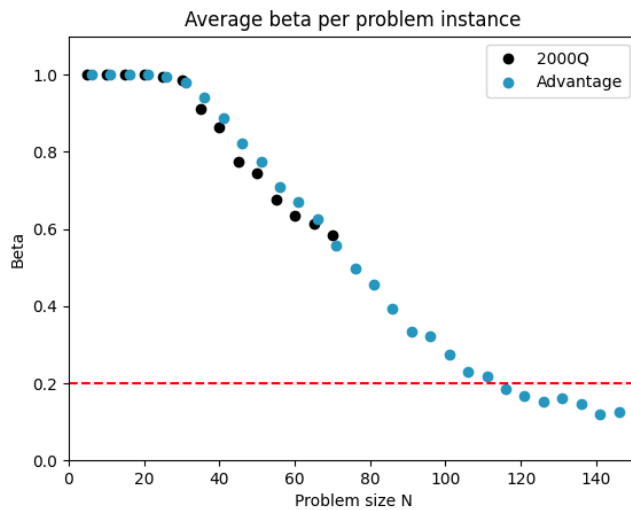


Figure 2: Max-Clique Q-score's  $\beta$  vs problem size  $N$ , with respect to optimal clique solution  $C_{max}$ , for the D-wave Advantage and 2000Q QPUs. For visibility reasons, the advantage graph is off-set by 1.

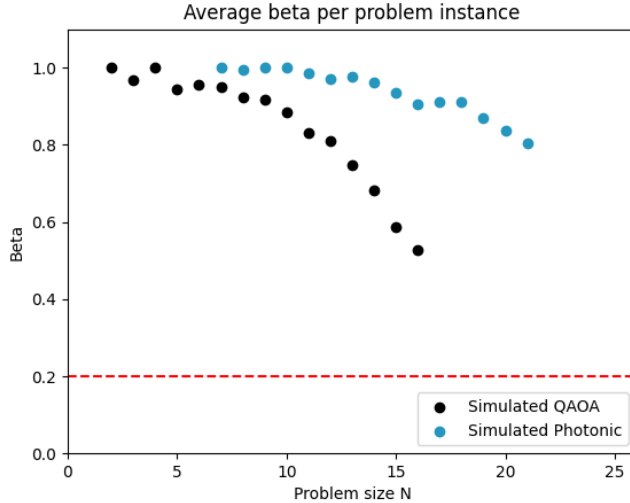


Figure 3: Max-Clique Q-score’s  $\beta$  vs problem size  $N$ , with respect to optimal clique solution as  $C_{max}$ , for noiseless simulations of gate-based quantum computing and photonic quantum computing.

Guadalupe and Starmon-5 devices, perfect clique solutions were found for all tested problem instances. Hence, both devices achieve  $\beta(N) = 1$  for all  $N \leq 5$ . The Starmon-5 device has five qubits, so no larger problem instances can be solved on this device. The Guadalupe device has sixteen qubits, but time-out errors in the experiments prevented computing the Max-Clique instances for  $N \geq 6$ .

Noiseless simulations have been performed up to problem sizes  $N = 16$  to upper-bound the achievable  $\beta$  on the Guadalupe device. Fig. 3 shows the  $\beta$  vs  $N$  graph. From the graph, we conclude that a Q-score Max-Clique of 16 is in principle attainable using the given QAOA setup.

- **Photonic quantum computing:** One of the leading companies in implementing physical boson sampling is Xanadu Quantum Technologies Inc. [39]. Their hardware however only allows bipartite graphs to be implemented. Instead, we use their boson sampling simulator to show upper-bound the  $\beta$  for a photonic approach. As boson sampling is difficult for classical computers to simulate, we were only able to do these simulations for graphs with problem sizes up to  $N = 20$  in reasonable time. Fig. 3 shows the  $\beta$  vs  $N$  graph.
- **Classical and hybrid:** Lastly, Fig. 4 shows the  $\beta$  vs  $N$  graph for D-wave’s classical and hybrid solvers. The simulations start for  $N = 100$  and increase in size with steps of 100. The computation is terminated

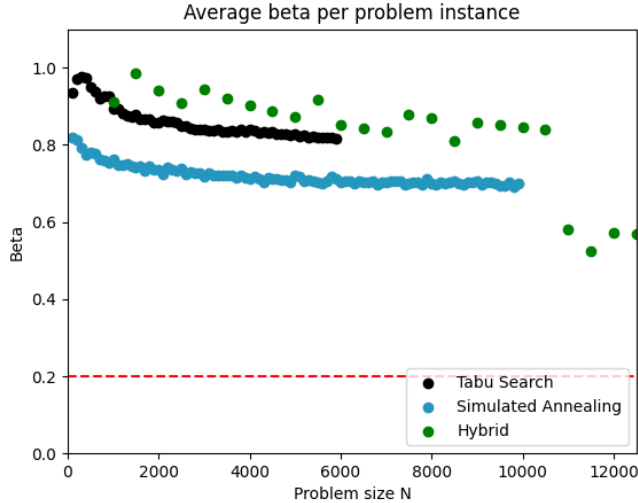


Figure 4: Max-Clique Q-score’s  $\beta$  vs problem size  $N$  for the D-wave classical tabu search solver (qbsolv), Simulated Annealing and their hybrid solver.

when the average time for graph sizes exceeds 100 seconds on our server to ensure that the region of 0 to 60 seconds is captured completely. For the hybrid solver, we calculated  $\beta$  for problem instances starting from  $N = 1,500$  up to  $N = 12,500$  with steps of 500 and a time constraint of 60 seconds. Due to the relative high cost of resources of the hybrid solver, only a single problem instance is considered. We expect that this lower bounds  $\beta$  for smaller problem instances.

Each of these solvers is able to maintain a  $\beta > 0.2$  for large problem instances  $N$ . Therefore, the Q-score Max-Clique is determined by the imposed 60 seconds time constraint. Fig. 5 shows the average time taken to solve a problem instance. For the hybrid solver, the minimum needed computation time is hard-coded. From these results, we report a Q-score Max-Clique of 9,100 and 4,900 for simulated annealing and tabu search respectively. The hybrid solver has a Q-score Max-Clique of 12,500 because of the hard-coded computation time constraint.

## 5 Discussion

In this work, we demonstrated that the Q-score metric, as originally introduced by Atos, extends to other optimisation problems. To compute a corresponding Q-score, such an extension requires a definition of a random algorithm and a corresponding asymptotic approximation of the optimal solution. Our choice for Max-Clique is motivated by the existence of a clique search algorithm for pho-

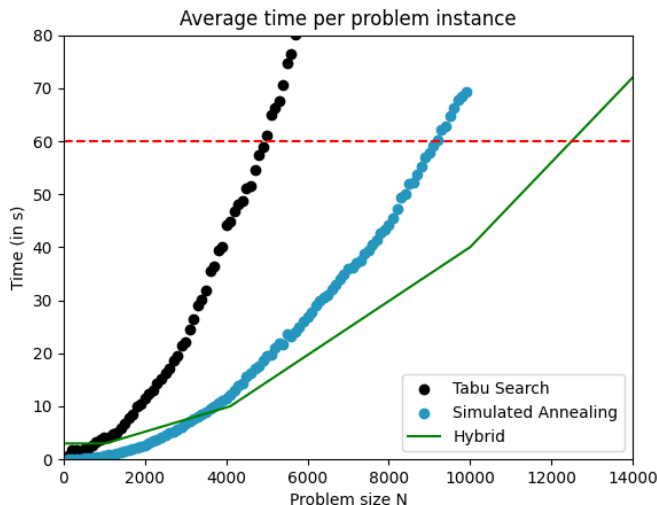


Figure 5: Average time taken per problem instance  $N$  for the D-wave classical tabu search solver (qbsolv), Simulated Annealing and the hybrid solver.

tonic hardware, hence allowing the metric to compare three different quantum computational paradigms.

Defining a Q-score metric inherently leaves a lot of freedom, even for a fixed optimisation problem. For instance, one could argue that our random algorithm choice is too naive resulting in a constant  $C_{rand}$  value, which might seem strange for large problem instances. A different, yet naive, algorithm would be to start from a random node and grow it to a clique by iterating over all possible vertices. In the end, different random algorithms will result in different  $\beta$  vs  $N$  graphs and hence different Q-scores. However, we expect that this does not significantly change the relative performance between devices.

Other degrees of freedom are the considered time constraint, the allowed pre- and post-processing optimisation steps, the value  $\beta^* = 0.2$  and even the considered optimisation problem. On the one hand, this forms a weakness of the Q-score metric: users should be very specific on how the metric is defined, which might complicate a potential comparison between different works. On the other hand, this also allows for different ways of benchmarking devices using a Q-score metric. A next step for the Q-score would be to consider a Q-score in which these degrees of freedom can be changed dynamically. The Q-score could hence be turned into a plug-and-play metric or suite of metrics suitable for benchmarking devices in a wide variety of ways.

In this work, the hybrid solver of D-Wave obtained the highest Q-score Max-Clique of 12,500 of all considered solvers. The differences with other classical solvers are however not yet significant enough to hint towards a quantum advantage. The hybrid solver forms a black box, which hinders attributing the better

performance solely to the quantum routines. Specifically, the hybrid solver uses a server stronger than our local solver for its classical routines. This inherently makes the comparison between the hybrid and classical solvers somewhat unfair. In addition, the  $\beta$  vs  $N$  graph for the hybrid solver shows a seemingly inexplicable drop at around  $N = 11000$ . It seems that there is something in the black box workings of the hybrid solver that results in problems of size larger than  $N = 10000$  being relatively more difficult to solve for the hybrid solver.

Quantum annealing has the largest Q-score Max-Clique of the different quantum computing approaches, with 110 for the Advantage system as its highest value. This is not a surprise as it has more qubits and hence allows for larger problems to be implemented than the considered gate-based hardware. We hope to compute Q-score Max-Clique on photonic hardware in the near future, as it will be an interesting comparison with current gate-based hardware. The noiseless simulations show that computing Q-score Max-Clique can indeed be done on photonic hardware. In turn, all classical solvers currently outperform the state-of-the-art quantum computers for each considered technology, as was originally expected.

Comparing Q-score Max-Clique with earlier results for Max-Cut [36], shows that the Q-score for the Advantage system is slightly lower (110 versus 140), while the 2000Q device finds the same score of 70 for both Q-scores. On the contrary, the classical approach performs better for the Max-Clique problem, with scores of 2,300 vs 4,900 and 5,800 vs 9,100 for tabu search and simulated annealing respectively. However, upon closer inspection we see that does not tell the whole story. Specifically, for the Q-score Max-Cut, the classical and hybrid solvers find solutions of perfect quality  $\beta = 1$  throughout, while for Q-score Max-Clique, the same solvers show both a variety and decrease in the solution quality parameter  $\beta$ . So, while the absolute Q-scores Max-Clique are higher, the Q-score Max-Cut finds higher quality solutions throughout. This hints towards the added value of a suite of Q-scores for different optimisation problems and parameter settings. In this way, the best hardware for each optimisation problem and application can be found.

For further work, it would be interesting to extend the QAOA results to more hardware backends and larger problem instances. For a fair comparison additional research is needed on the execution time of QAOA. Alternatively, it would also be interesting to consider different gate-based algorithm approaches. For example, one could also solve the Max-Clique problem using a Grover's search [20].

## References

- [1] Scott Aaronson and Alex Arkhipov. The computational complexity of linear optics. *Theory of Computing*, 9(4):143–252, 2013.
- [2] Dorit Aharonov. A simple proof that Toffoli and Hadamard are quantum universal, 2003.

- [3] Dorit Aharonov, Wim van Dam, Julia Kempe, Zeph Landau, Seth Lloyd, and Oded Regev. Adiabatic quantum computation is equivalent to standard quantum computation. *SIAM Journal on Computing*, 37(1):166–194, January 2007.
- [4] Juan Miguel Arrazola and Thomas R. Bromley. Using Gaussian boson sampling to find dense subgraphs. *Physical Review Letters*, 121(3), jul 2018.
- [5] Leonardo Banchi, Mark Fingerhuth, Tomas Babej, Christopher Ing, and Juan Miguel Arrazola. Molecular docking with Gaussian boson sampling. *Science Advances*, 6(23):eaax1950, 2020.
- [6] R. Barends, J. Kelly, A. Megrant, D. Sank, E. Jeffrey, Y. Chen, Y. Yin, B. Chiaro, J. Mutus, C. Neill, P. O’Malley, P. Roushan, J. Wenner, T. C. White, A. N. Cleland, and John M. Martinis. Coherent Josephson qubit suitable for scalable quantum integrated circuits. *Phys. Rev. Lett.*, 111:080502, Aug 2013.
- [7] Jerry M. Chow, Jay M. Gambetta, A. D. Córcoles, Seth T. Merkel, John A. Smolin, Chad Rigetti, S. Poletto, George A. Keefe, Mary B. Rothwell, J. R. Rozen, Mark B. Ketchen, and M. Steffen. Universal quantum gate set approaching fault-tolerant thresholds with superconducting qubits. *Phys. Rev. Lett.*, 109:060501, Aug 2012.
- [8] J. I. Cirac and P. Zoller. Quantum computations with cold trapped ions. *Phys. Rev. Lett.*, 74:4091–4094, May 1995.
- [9] Andrew W. Cross, Lev S. Bishop, Sarah Sheldon, Paul D. Nation, and Jay M. Gambetta. Validating quantum computers using randomized model circuits. *Phys. Rev. A*, 100:032328, Sep 2019.
- [10] Christoph Dankert, Richard Cleve, Joseph Emerson, and Etera Livine. Exact and approximate unitary 2-designs and their application to fidelity estimation. *Phys. Rev. A*, 80:012304, Jul 2009.
- [11] Philippe Duluc, Pierre-Antoine Harraud, Ewan Munro, and Joaquin Keller. How quantum technology will revolutionize healthcare. *Atos Ascent Magazine*, 2019.
- [12] Joseph Emerson, Robert Alicki, and Karol Życzkowski. Scalable noise estimation with random unitary operators. *Journal of Optics B: Quantum and Semiclassical Optics*, 7(10):S347–S352, September 2005.
- [13] Paul Erdős and Alfréd Rényi. On the evolution of random graphs. *Publ. Math. Inst. Hung. Acad. Sci*, 5(1):17–60, 1960.
- [14] Paul Erdős and Alfréd Rényi. On random graphs. *Publ. Math. Debrecen*, 6:290–297, 1959.

- [15] Edward Farhi, Jeffrey Goldstone, and Sam Gutmann. A quantum approximate optimization algorithm, 2014.
- [16] Edward Farhi, Jeffrey Goldstone, Sam Gutmann, and Michael Sipser. Quantum computation by adiabatic evolution, 2000.
- [17] Fred Glover. Tabu search—part i. *ORSA Journal on Computing*, 1(3):190–206, August 1989.
- [18] Fred Glover. Tabu search—part II. *ORSA Journal on Computing*, 2(1):4–32, February 1990.
- [19] Fred W. Glover and Gary A. Kochenberger. A tutorial on formulating QUBO models. *CoRR*, abs/1811.11538, 2018.
- [20] A. Haverly and S. López. Implementation of Grover’s algorithm to solve the maximum clique problem. In *2021 IEEE Computer Society Annual Symposium on VLSI (ISVLSI)*, pages 441–446, 2021.
- [21] Andrew R. Haverly. A comparison of quantum algorithms for the maximum clique problem. Master’s thesis, Rochester Institute of Technology., 5 2021.
- [22] A. A. Houck, Jens Koch, M. H. Devoret, S. M. Girvin, and R. J. Schoelkopf. Life after charge noise: recent results with transmon qubits. *Quantum Information Processing*, 8(2-3):105–115, February 2009.
- [23] Tadashi Kadowaki and Hidetoshi Nishimori. Quantum annealing in the transverse Ising model. *Phys. Rev. E*, 58:5355–5363, Nov 1998.
- [24] A Yu Kitaev. Quantum computations: algorithms and error correction. *Russian Mathematical Surveys*, 52(6):1191–1249, December 1997.
- [25] Thomas Lubinski, Sonika Johri, Paul Varosy, Jeremiah Coleman, Luning Zhao, Jason Necaie, Charles H. Baldwin, Karl Mayer, and Timothy Proctor. Application-Oriented Performance Benchmarks for Quantum Computing, 2021.
- [26] Andrew Lucas. Ising formulations of many NP problems. *Frontiers in Physics*, 2, 2014.
- [27] Vladimir E. Manucharyan, Jens Koch, Leonid I. Glazman, and Michel H. Devoret. Fluxonium: Single Cooper-pair circuit free of charge offsets. *Science*, 326(5949):113–116, 2009.
- [28] Simon Martiel, Thomas Ayril, and Cyril Allouche. Benchmarking quantum coprocessors in an application-centric, hardware-agnostic, and scalable way. *IEEE Transactions on Quantum Engineering*, 2:1–11, 2021.
- [29] David W Matula. *The largest clique size in a random graph*. Department of Computer Science, Southern Methodist University Dallas, Texas, 1976.



- [30] Elijah Pelofske, Georg Hahn, and Hristo Djidjev. Solving large maximum clique problems on a quantum annealer. In *Quantum Technology and Optimization Problems*, pages 123–135. Springer International Publishing, 2019.
- [31] A. Politi, J. Matthews, M.G. Thompson, and J.L. O'Brien. Integrated quantum photonics. *IEEE Journal of Selected Topics in Quantum Electronics*, 15(6):1673–1684, 2009.
- [32] IBM Quantum. ibmq\_guadalupe. [https://quantum-computing.ibm.com/services/resources?tab=systems&view=grid&system=ibmq\\_guadalupe](https://quantum-computing.ibm.com/services/resources?tab=systems&view=grid&system=ibmq_guadalupe).
- [33] IBM Quantum. Qiskit runtime. <https://quantum-computing.ibm.com/lab/docs/iql/runtime/>.
- [34] TNO Quantum. TNO Quantum / qscore. <https://github.com/TNO-Quantum/qscore>.
- [35] QuTech. Quantum inspire starmon-5 fact sheet. <https://www.quantum-inspire.com/backends/starmon-5/>, 6 2020.
- [36] Ward van der Schoot, Daan Leermakers, Robert S. Wezeman, Niels M. P. Neumann, and Frank Phillipson. Evaluating the Q-score of quantum annealers. *2022 IEEE International Conference on Quantum Software (QSW)*, pages 9–16, 2022.
- [37] Andrew Wack, Hanhee Paik, Ali Javadi-Abhari, Petar Jurcevic, Ismael Faro, Jay M. Gambetta, and Blake R. Johnson. Quality, speed, and scale: three key attributes to measure the performance of near-term quantum computers. *arXiv preprint arXiv:2110.14108v2*, 2021.
- [38] Johannes Weidenfeller, Lucia C. Valor, Julien Gacon, Caroline Tornow, Luciano Bello, Stefan Woerner, and Daniel J. Egger. Scaling of the quantum approximate optimization algorithm on superconducting qubit based hardware. *Quantum*, 6:870, dec 2022.
- [39] Xanadu. Welcome to Xanadu. <https://www.xanadu.ai/>.